Computational and Structural Biotechnology Journal 21 (2023) 3875–3884

Contents lists available at ScienceDirect

Computational and Structural Biotechnology Journal

journal homepage: www.elsevier.com/locate/csbj

Research article

Synergetic effect of β-asarone and cannabidiol against Aβ aggregation *in vitro* and *in vivo*

Fangyuan Duan [a,c], Ting Ju [a,c], Chen Song [a,c], Mengyao Liu [a,c], Yi Xiong [a,c], Xue Han [b], Weihong Lu [b,c,d,*]

[a] School of Chemistry and Chemical Engineering, Harbin Institute of Technology, Harbin 150001, China
[b] School of Medicine and Health, Harbin Institute of Technology, Harbin 150001, China
[c] National and Local Joint Engineering Laboratory for Synthesis, Transformation and Separation of Extreme Environmental Nutrients, Harbin 150001, China
[d] The Intelligent Equipment Research Center for the Development of Special Medicine and Food Resources, Chongqing Research Institute of HIT. Harbin Institute of Technology, Chongqing 401120, China

ARTICLE INFO

Keywords:
β-asarone
CBD
Alzheimer's disease
Amyloid β
Phytochemicals
C. elegans

ABSTRACT

Alzheimer's disease (AD) is a complex and multifactorial neurodegenerative disorder, and it is unlikely that any single drug or intervention will be very successful. The pathophysiology of Alzheimer's disease involves a range of complicated biological processes, including the accumulation of beta-amyloid protein and tau protein. Given the complexity of AD and amyloid accumulation, a combination of interventions remains to be further explored. Here, we investigated the potential of combining β-asarone and cannabidiol (CBD) as a treatment for AD. The study analyzed the combined effects of these two phytochemicals on beta-amyloid (Aβ) protein aggregation and toxicity in bulk solution, in cells as well as in *C.elegans*. We detailed the morphological and size changes of $A\beta_{40}$ aggregates in the presence of β-asarone and cannabidiol. More importantly, the presence of both compounds synergistically inhibited apoptosis and downregulated relative gene expression in cells, and that it may also slow aging, decrease the rate of paralysis, enhance learning capacity, and boost autophagy activity in *C.elegans*. Our studies suggest that multiple drugs, like β-asarone and CBD, may be potentially developed as a medicinal adjunct in the treatment of AD, although further clinical trials are needed to determine the efficacy and safety of this combination treatment in humans.

1. Introduction

Alzheimer's disease (AD) is a complex neurodegenerative disorder with multiple underlying mechanisms. The disease is manifested by the presence of beta-amyloid (Aβ) plaques and tau tangles in the brain [1,2]. Reducing their burden is a key target for developing more effective drugs against the disease. Therapeutics inhibiting Aβ production or deposition are being investigated, such as beta-secretase inhibitors [3], gamma-secretase inhibitors [4], and immunotherapy [1,5] targeting Aβ. In addition, drugs that modulate Aβ and tau pathology, neuroinflammation, oxidative stress, and synaptic dysfunction are also being explored. However, clinical trials of these drugs are still under debate so far. It is highly plausible that this main challenge is caused by the complicated amyloid aggregation and their significant consequences on cellular and subcellular functions. To overcome this challenge, combination therapies may shed light on simplifying the complexity. There are some researches about combination of two or more medicine to have a better result than the single one [6,7].

Cannabidiol (CBD) and β-asarone are both phytochemicals with diverse studies in neurodegenerative diseases. CBD is a non-psychoactive phytocannabinoid [8] derived from the plant Cannabis sativa. CBD prevents cognitive impairment in AD mouse model [9] and is able to modulate different receptors in the endocannabinoid system [10]. On the other hand, β-asarone has been found to have a significant therapeutic effect against toxic protein deposition [11], inhibit Aβ by promoting autophagy [11], and weaken apoptosis [12]. Either CBD or β-asarone has the researches to cooperate with other components to work on neurodegenerative diseases. While during these studies, CBD only worked with THC and β-asarone only worked with levodopa when they work in Parkinson's disease [13–15], for AD, there will be more combination trials, such as Icariin [16], tenuigenin [17] and eugenol [18]. But there is no research about the combination of them two or

* Correspondence to: School of Chemistry and Chemical Engineering, Harbin Institute of Technology, A1003 Mingde Building, Harbin 150001, China.
E-mail address: lwh@hit.edu.cn (W. Lu).

https://doi.org/10.1016/j.csbj.2023.07.028
Received 5 May 2023; Received in revised form 17 July 2023; Accepted 19 July 2023
Available online 28 July 2023

showing the precise influence on morphology of $A\beta_{40}$. This is the first trial to combine CBD and β-asarone, which are phytochemicals with similar structure, so we carried out the experiment with a ratio of 1:1 of them.

C. elegans is an effective model to study relationship between neurodegenerative processes with drug targets [19]. CL4176 strains of *C. elegans* to investigate the effects of the two compounds on aging and AD. N2 is a wild-type strain of *C. elegans*, while CL4176 is a transgenic strain that expresses $A\beta_{1-42}$ and exhibits paralysis as a result of Aβ toxicity [20]. The increasing level of Aβ and p-tau will lead to loss of cognitive function [21], especially soluble Aβ oligomers will aggravate disease progression [22], so in this paper, we used two $A\beta_{1-42}$ over-expressed *C.elegans*.

In this study, we investigate if the progression of AD could be slowed down through the combination of the two compounds. The morphologies of AFM showed clearly that the two phytochemicals could decrease the height and the length of the $A\beta_{40}$ aggregates. We implemented *C. elegans* and SH-SY5Y cells to investigate the effects of β-asarone and CBD on the aging process and the development of Aβ. The combination of these two compounds was able to extend the lifespan and alleviate paralysis caused by Aβ in CL4176 *C.elegans* model.

2. Materials and methods

2.1. Differential expression genes determination

Differential expressed genes were obtained to see how these genes changed in our cell model after having the two phytochemicals treatment. In brief, GSE97760 dataset was analyzed by limma package from Bioconductor to search for differently expressed genes (DEGs). As the clinical data showed more than 2000 DEGs existed between AD and healthy people, and CBD is mostly studied with endocannabinoid system [23,24], then genes related to retrograde endocannabinoid system in KEGG (Kyoto Encyclopedia of Genes and Genomes) was intersected to obtain target genes (Supplement Fig. 1B).

2.2. Chemicals

β-asarone (purity ≥98 %) was from Macklin, and CBD (purity ≥99 %) was from Harbin Smart/Intelligent Industrial Hemp Industry Development Co., Ltd. (http://www.hitsmarthemp.com/). Dimethyl sulfoxide (DMSO) was from Sigma (USA). BV2 and SH-SY5Y cells were provided by Cell Resource Center, Institute of Basic Medical Sciences, CAMS/PUMC (Beijing, China). Dulbecco modified eagle medium (DMEM) and Roswell Park Memorial Institute (RPMI-1640) were from Gibco (Shanghai, China). Fetal bovine serum (FBS) was from Clark Bioscience and penicillin-streptomycin was from Beyotime. Polyvinylidene difluoride (PVDF) membrane was from Millipore (USA). Antibodies to LC3 and Bcl-xl were purchased from Cell Signaling Technology, Inc. (Danvers, MA, USA). P62 was purchased from Sigma (Shanghai, China). Tubulin was purchased from Cusabio. All other reagents were of analytical grade. As some researchers showed that different reagents would benefit for Alzheimer's disease model [25], for example, some DMSO concentrations prevent apoptosis whereas higher concentrations induce apoptosis [26] *in vitro* experiment [27], and mouse embryos [28]. Then DMSO in all the experiments in this article would be adjusted to the same concentration *in vivo/in vitro* assays to avoid solvent influence (0.4 % *in vitro* experiment, and 0.2 % in *vivo* experiment).

2.3. C. elegans strains

CL4176 dvIs27 [myo-3p::A-Beta (1-42)::let-851 3′UTR) + rol-6 (su1006)], CL2355 dvIs50 [pCL45 (snb-1::Abeta 1–42::3′ UTR(long) + mtl-2::GFP], N2 and *Escherichia coli* strain (OP50) were from the Caenorhabditis Genetics Center (CGC, University of Minnesota, America). According to standard procedures, *C. elegans* was cultivated at 16 °C or 25 °C on a standard nematode growth medium (NGM) seeded with OP50 for food [29].

2.4. Cell assays

Transgenic mice that express FAD mutant APP and PS1 overproduce Aβ42 and exhibit amyloid plaque pathology similar to that found in AD [30]. APP and PSEN1 were constructed in the plasmid and connected with a linker P2A [31]. The cells in the logarithmic growth phase were seeded into the 6-well plates and were transfected according to the instructions of the transfection reagent (TransGen Biotech, Beijing, China). Transfection was conducted by the plasmid for 24–48 h, then were exposed to different concentrations of β-asarone, CBD, or a combination of them for another 24 h after adding transfect agent. Cell viability rates were subsequently assessed using the cell counting kit-8 (CCK-8) (Bimake, Beijing, China) according to the manufacturer's instructions.

2.5. Worm behavior assays

The worms were synchronized with sodium hypochlorite and maintained in NGM plates (with or without β-asarone, CBD, or the combination of the two drugs) at 16 or 25 °C until they reached the specific stage larvae.

Lifespan assay was performed as the previous report with minor modifications [32]. In brief, the CL4176 worms were treated as described above and turned into adult, then transferred to 25.5 °C, and the dead worms were scored every day by gentle prodding of the anterior end of the worm body with a platinum wire. The survival time was calculated after they were moved to 25.5 °C, and the survival curves represent the percentage of nematodes that were considered alive at the relevant time points. All the lifespan experiments were repeated three times (30 worms in each group).

Paralysis assay was performed as the report with minor modifications [33,34]. Briefly, the paralysis nematodes were transferred to 25.5 °C for 24 h and counted every 2 h after L3 or every day after L4. The nematodes that can only move their heads were marked as paralyzed (at least 30 worms in each group).

Pharyngeal pumping assay was taken into record with observable pumping activity using microscope (Leica S6, Germany) for 30 s. The mean number of pumps were plotted with 13–28 worms for each group.

Head Thrashing Assay was performed as follows, with slight modifications [35]. After the worms reached L4 incubated with different combinations, then transferred to an unseeded plate, 10 μL M9 buffer was added on the worms. The number of head thrashes was counted with 6–10 worms for each group.

Chemotaxis index was measured as follows with a little modifications [36]. Briefly, after synchronization, 30–100 eggs were randomly placed into different condition plates for 1 h at room temperature. Different concentrations of CBD or β-asarone were put on the Test points with 2 μL, and the Control points were placed with solution of them.

$$\text{Chemotaxis Index (CI)} = [\text{nTest A}+\text{nTest B}]/[\text{nControl C}+\text{nControl D}].$$

Long-term learning ability was measured by the odorant preference assay with some modifications [37]. Briefly, the age-synchronized worms were maintained in NGM plates at 20 °C until they were grown to the young adults, which were collected with M9 buffer and washed 3 times to remove bacteria. Synchronized worms were harvested and divided into naive and trained groups. Each group was performed in triplicate and contained about 50–300 worms. The worms were starved in M9 buffer at room temperature for 1 h before the assay. Conditioning block means incubating conditioning plates at room temperature for 30 min and starve block means starving in a 15 mL centrifuge tube at room temperature for 30 min. The assay contains 7 conditioning blocks

and 6 starve blocks. Incubate post-conditioning plates for 16 h (long--term associative memory time points) at 20 °C. The number of worms was counted on both butanone and ethanol spots after 1 h.

Chemotaxis Index (CI) = [(nButanone)-(nEtOH)]/[(Total-nOrigin)].

Learning Index (LI) = $CI_{Timepoint} - CI_{Naive}$.

2.6. Fluorescence measurement

Apoptosis was conducted as followed, cells first were stained by Annexin-mCherry kit and then Hoest3342, which represented the living cell nuclei. Transfect ratio ofAPP/PS1 plasmid in cells was observed according to the green fluorescence density.

In vivo experiment, we used *C.elegans* to conduct amyloid aggregation situations and the mitochondria. The amyloid aggregation was conducted by the Th-S staining method from the modified staining method [38]. In brief, the synchronous nematodes were obtained followed standard method [39] and were incubated with Th-S at the young-adult stage. The worms were washed and anesthetized by the addition of 2 mM levamisole.

Mitochondrial Membrane Potential Assay. Prepared CL4176 worms with different treatments. After the addition of PBS (Sigma-Aldrich, Milan, Italy) and mitochondrial membrane potential (MMP) probe JC-1 (10 μM) (Solarbio, Beijing, China), worms were incubated for 1 h in darkness, followed by labeling through the fluorescent. And the anesthesia was taken before observation to make sure the worms were still alive. To obtain the ratio of red to green fluorescence intensity, worms were assessed through confocal fluorescence ratio imaging by laser scanning confocal microscope (LSCM) (Olympus). The images were taken at ten folds magnification. Fluorescence intensities were assessed using Image J, and three independent experiments were performed.

2.7. Dynamic light scattering (DLS) analysis

To characterize the size distribution status of amyloid β after ThT binding assay, we applied DLS analysis using Prometheus (NanoTemper, Germany) at 37 °C. Each sample has ten repeat measurements to check the result repeatability.

2.8. Western blot analysis

Western blotting analysis was performed following the procedure in the previous report with minor modifications [40]. The treated cells were washed twice with PBS, and then the total protein extracts were isolated using protein extraction commercial kits, which had been collected and treated as mentioned above. The concentration of total protein in stored at −80 °C. Proteins were separated by SDS-PAGE (12 %) and transferred to PVDF membranes. The protein bands were detected using the Enhanced ECL Western Blotting Kit (GE Healthcare, Munich, Germany). Relative optical densities and areas of ban were quantified using the Quantity One software. The densitometry plots of the results were normalized to the intensity of the β-actin band. Protein contents were assessed according to the BCA protein quantity kit (Beyotime, Shanghai, China).

2.9. Quantitative real-time PCR

Total RNA was isolated and remove residual genomic DNA was removed using the TaKaRa MiniBEST Universal RNA Extraction Kit (Takara Bio, Dalian, China) according to the manufacturer's guidelines after fracturing the cells containing Protease Inhibitor Cocktail and Phosphatase Inhibitor Cocktail (both from Bimake, Houston, TX, USA). According to the manufacturer's guidelines, complementary DNA was synthesized from 1 μg total RNA using a PrimeScriptTM RT reagent Kit (Takara Bio, Dalian, China) and temporarily stored at −80 °C. qRT-PCR was conducted using SYBR Premix Ex Taq TM II (Takara Bio, Dalian, China) with a CfX 96 Connect™ system (Bio-Rad, Munich, Germany). Primers were purchased from BioMers (Sangon Biotech, China). Oligonucleotide primer sequences, primer concentrations, and product sizes are listed in Table 1. PCR cycling conditions were an initial denaturation at 95 °C for 3 min, followed by 45 cycles of 95 °C for 10 s, 58 °C for 45 s (except for aak-2 at 62 °C), and extension at 72 °C for 29 s. Gene expression levels were analyzed by applying the –(2ΔΔCq) and normalized to the expression levels of amanitin resistant (ama-1) and actin (act-2).

2.10. Atomic force microscopy (AFM)

Prior to imaging, an aliquot (10 μL) For each sample analysis, 10 μL of the reaction mixture got from ThT binding assay were deposited in freshly cleaved mica sheets and allowed to dry for a minimum of 10 min. After that, the mica sheets were gently washed with Milli-Q water. The mica sheets were then dried with air flow for 5 min [41] and visualized using atomic force microscope (Bruker, USA). Images were acquired with Tapping mode in Air mode. Samples were probed at different scanning sizes (from 1 μm to 3 μm), with 840 or 1024 lines/image and scanning rates of either 0.50 Hz/line. The images are flattened using Gwyddion software and no further image processing was carried out.

For AFM measurement in air, 10 μM Aβ40, with or without coaggregates (1 %, 10 %) were obtained from ThT Assay. 10 μL of each sample was then added onto the freshly cleaved muscovite mica (Electron Microscopy Sciences) and incubated for 8 min at room temperature. The excess sample was removed with 150 μL of Milli-Q water and dried under nitrogen gas. The images were obtained with the Bruker Dimension Icon Scanning Station (Bruker, USA) in intermittent tapping mode in air and processed with Gwyddion [42]. The height values of the grains were taken to provide histograms, mean and error values using Origin.

2.11. THT binding assay

To investigate the effect of combination of the two phytochemicals inhibition activity of $A\beta_{40}$ aggregation by thioflavin T (ThT) fluorescence assay in 384 well plates, β-asarone and CBD were conducted with a modification [43]. In brief, the $A\beta_{40}$ (10 μM) was incubated with compounds in different concentrations for 16 h in phosphate buffer (PB, 20 mM, pH 7.4) containing 50 μM ThT. The control wells were filled with an equal amount of vehicle DMSO. All samples were prepared on ice, and 35 μL of each sample was transferred into a 384-well black plate with transparent bottom (NUNC) and sealed with foil film. The plate was incubated in a microplate reader (PHERAstar FSX, BMG LABTECH, Germany) and the fluorescence kinetics of $A\beta_{40}$ was monitored at 37 °C with agitation every 10 min, using wavelengths of 430 nm and 480 nm for excitation and emission, respectively.

All of the original ThT data were plotted with Origin (Version 2019, OriginLab, USA). The averaged ThT data were normalized as previous

Table 1
Phenomenological paramerters for $A\beta_{40}$ aggregation (t_{lag}, t_{half}, h), calculated from the sigmoidal curve fitting of the ThT fluorescence kinetic assay.

	Concentration	t_{lag} (h)	t_{half} (h)
Aβ40	10 μM	8.11 ± 0.01	9.8 ± 0.01
β-asarone+	25 μg/mL	10.19 ± 0.01	11.49 ± 0.01
Aβ40	5 μg/mL	9.37 ± 0.01	10.86 ± 0.01
	2.5 μg/mL	9.90 ± 0.02	11.25 ± 0.03
CBD+Aβ40	25 μg/mL	11.21 ± 0.01	12.76 ± 0.02
	5 μg/mL	10.21 ± 0.01	11.56 ± 0.02
	2.5 μg/mL	9.59 ± 0.01	10.94 ± 0.01
β-asarone+ CBD+Aβ40	25 μg/mL+ 25 μg/mL	11.02 ± 0.01	12.47 ± 0.02
	5 μg/mL+ 5 μg/mL	9.48 ± 0.01	11.03 ± 0.02
	2.5 μg/mL+ 2.5 μg/mL	9.99 ± 0.01	11.70 ± 0.01

work [44], the half time, $t_{1/2}$ [45] was obtained by fitting a sigmoidal function to each kinetic trace shown with Eq. (1), and the lag time, t_{lag}, was defined as Eq. (2).

$$y = y_0 + \frac{(y_{max} - y_0)}{(1 + \exp(-k(t - t_{1/2}))} \quad (1)$$

$$t_{lag} = t_{1/2} - 2/k \quad (2)$$

2.12. Statistical analyses

Statistical analyses were performed using GraphPad Prism 5™. One-way analysis of variance (ANOVA) followed by the Turkey test was used for statistical evaluation of the antioxidant activities. For lifespan studies, P values were derived from log-rank calculations. All determinations were represented as Mean ± SEM and $P < 0.05$ was considered to indicate statistical significance.

3. Results

3.1. Synergetic effects of CBD and β-asarone on gene expression and improve the cytotoxicity in vitro

First, we wanted to test how the two compounds work on the Aβ aggregation by using ThT binding assay and the kinetic was conducted for 16 h (Fig. 1A). The fluorescence intensity clearly decreased when combine the two compounds at 5 μg/mL. These data were globally analyzed by the AmyloFit online software server [46]. We could see that either β-asarone or CBD inhibited $A\beta_{40}$ aggregation compared to Aβ alone and the highest concentration had the highest inhibitory activity (Supplement Fig. 1A), while β-asarone might not present too much dose-dependent ability and the inhibition activity of CBD itself will be hugely dose-dependent. Our sigmoidal curve fitting reveals that both the lag time and half time of $A\beta_{40}$ aggregation were prolonged with the addition of the two compounds (Table 1). And when we combined the two compounds together, the low dosage (2.5 μg/mL of each) could have a better inhibition when compared to the medium dosage (5 μg/mL of each), which could confirm our hypothesis that the combination of two compounds would work better in lower dosage and have the possibility to get rid of the harm caused by high dosage. While, CBD single use could have a better inhibitory effect on $A\beta_{40}$ fibrillization compared to combined.

Then, we wanted to test if the combined treatment could have a better effect in cells, we transfected plasmid to construct a cell model. After the transfection, we measured the cell viability of the SH-SY5Y cell model, which was widely used as an *in vitro* model in PD research [47] with a single compound or combination in different concentrations. It was easy to see that (Fig. 1B) CBD could be toxic (25 μg/mL) to cells and β-asarone could attenuate the toxicity in the combined groups. And the low dosage group (with 2.5 μg/mL) had the most efficient ability to

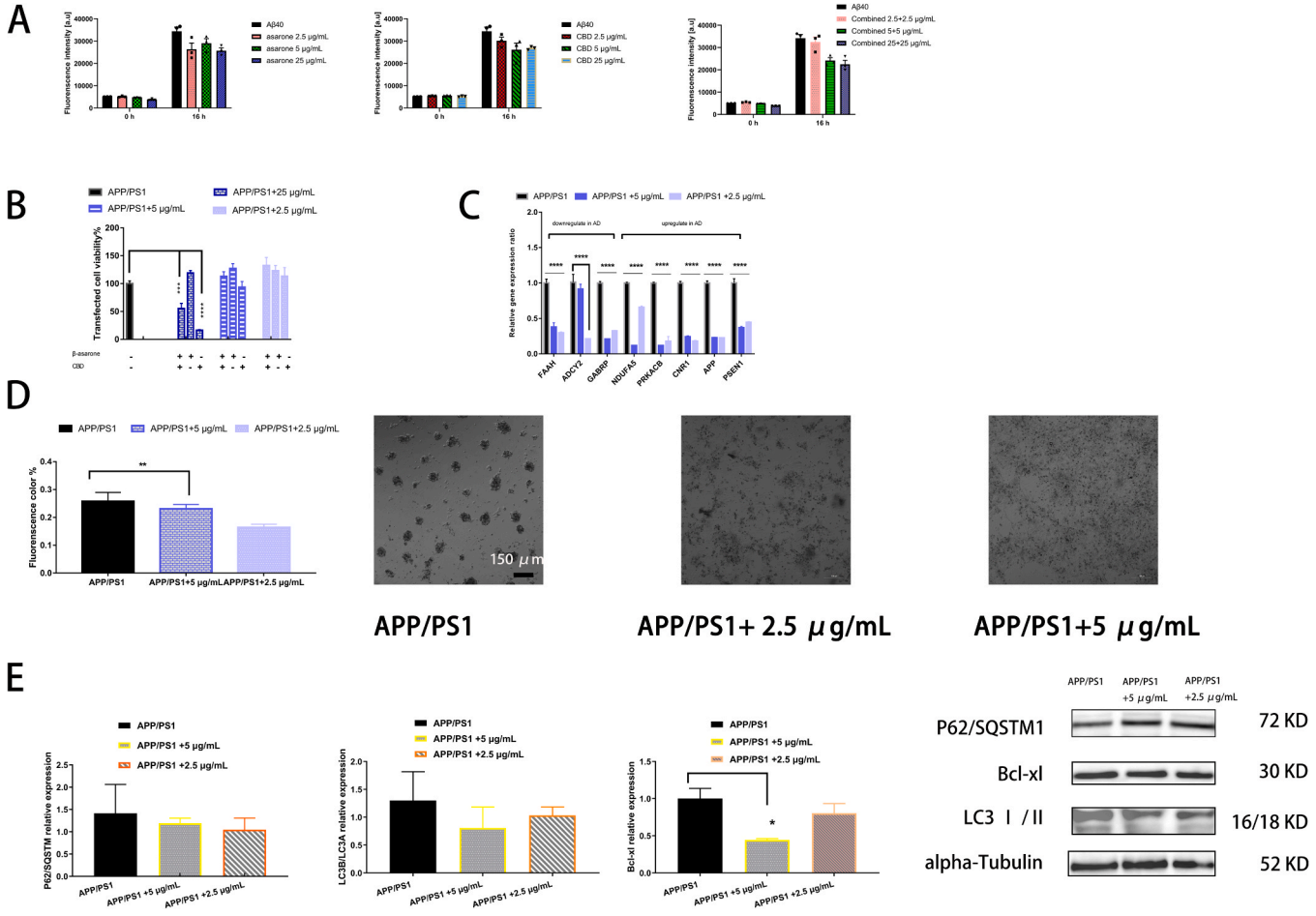

Fig. 1. The effect of CBD and β-asarone on Aβ fibrillization. (A) Fluoresene intensity for $A\beta_{40}$ with two phytochemicals. Aggregation was monitored in the presence of 20 μM ThT in 20 mM phosphate buffer with 10 μM Aβ40 at pH 7.4 for different concentrations. (B) Cell viability of the combination of CBD and β-asarone in transfected SH-SY5Y cell model. (C) Gene expressions in SH-SY5Y cell model after transfection. (D) Morphology of the transfected cells with or without the combination dosages and the fluorescent signal of them. Scale bar: 150 μm. (E) Autophagy protein expression influenced by the combination of CBD and beta-asarone in transfetced cell model. All proteins were analyzed by one-way ANOVA with 3 replicates.

improve cell viability. As the plasmid contained GFP signal and the transfect process or the express of the plasmid would be harmful to the cells, confocal images were taken after with or without the two phytochemical combination treatment for another 24 h.

As Aβ not only appeared in senile area, but also will appeared in arteriolar blood vessel walls [48]. Then, it is useful to investigate how genes expression changed in blood to detect disease process. In that case, we selected a GEO dataset, which studied blood gene changes and retrograde endocannabinoid signaling pathway to select target genes. There were 6 genes that appeared differentially changed, which were PRKACB, ADCY2, NDUFA5, CNR1, GABRP, FAAH (Supplement Fig. 1B). After that, selected genes were analyzed by qRT-PCR (Fig. 1 C). The 6 genes were all downregulated after having two phytochemicals cultivated, FAAH and ADCY2, which were downregulated in AD patients and had a little upregulation effect. It was easy to see (Fig. 1 D) that cells in the control group (0.2 % DMSO) were in an unhealthy condition, all the cells were in clusters, while the cells stayed in good condition after the dosage of the combination of the 2 phytochemicals, which we believed that the combination treatment could reverse the side effect caused by the transfection.

3.2. Synergetic effects of two phytochemicals on autophagy/apoptosis induced by APP/PS1

Autophagy has a strong relationship with AD with so many researches have proved that [49–52]. Here we used three major autophagy related proteins to test what have changed in the cell model with or without the compounds. SQSTM1, which is associated with autophagy and correlates with ubiquitinated proteins aimed at autophagy degradation [53] and reduced deposition of $A\beta_{42}$, $A\beta_{40}$, and amyloid precursor protein (APP) in the hippocampus of the AD animal model [54]. To test the effect of the combination of the two compounds on autophagy flux, SH-SY5Y cells were treated with medium (5 μg/mL) and low concentration (2.5 μg/mL) 48 h after transfection. Bcl-xl, LC3B/A and p62 were simultaneously detected by western blotting. The result showed that the combination treatment modulated the autophagy in SH-SY5Y cells (Fig. 1 E). CBD might be the reason that decreased LC3-II/LC3-I but increased SQSTM1, which was opposite to the research [55], but similar to the research [54]. In the medium group, LC3 II/I ratio and the Bcl-xl were both downregulated approximate 49 % and 55 %, respectively, which meant the combination treatment could reduce the deposition of toxic proteins. While P62/SQSTM1 was slightly decreased when compared to the control group, which meant it might be digested during autophagy.

3.3. The morphology and insight status of $A\beta_{40}$ caused by CBD and β-asarone

The size distribution of the mixture after ThT binding assay was directly performed by dynamic light scattering (DLS). DLS analysis

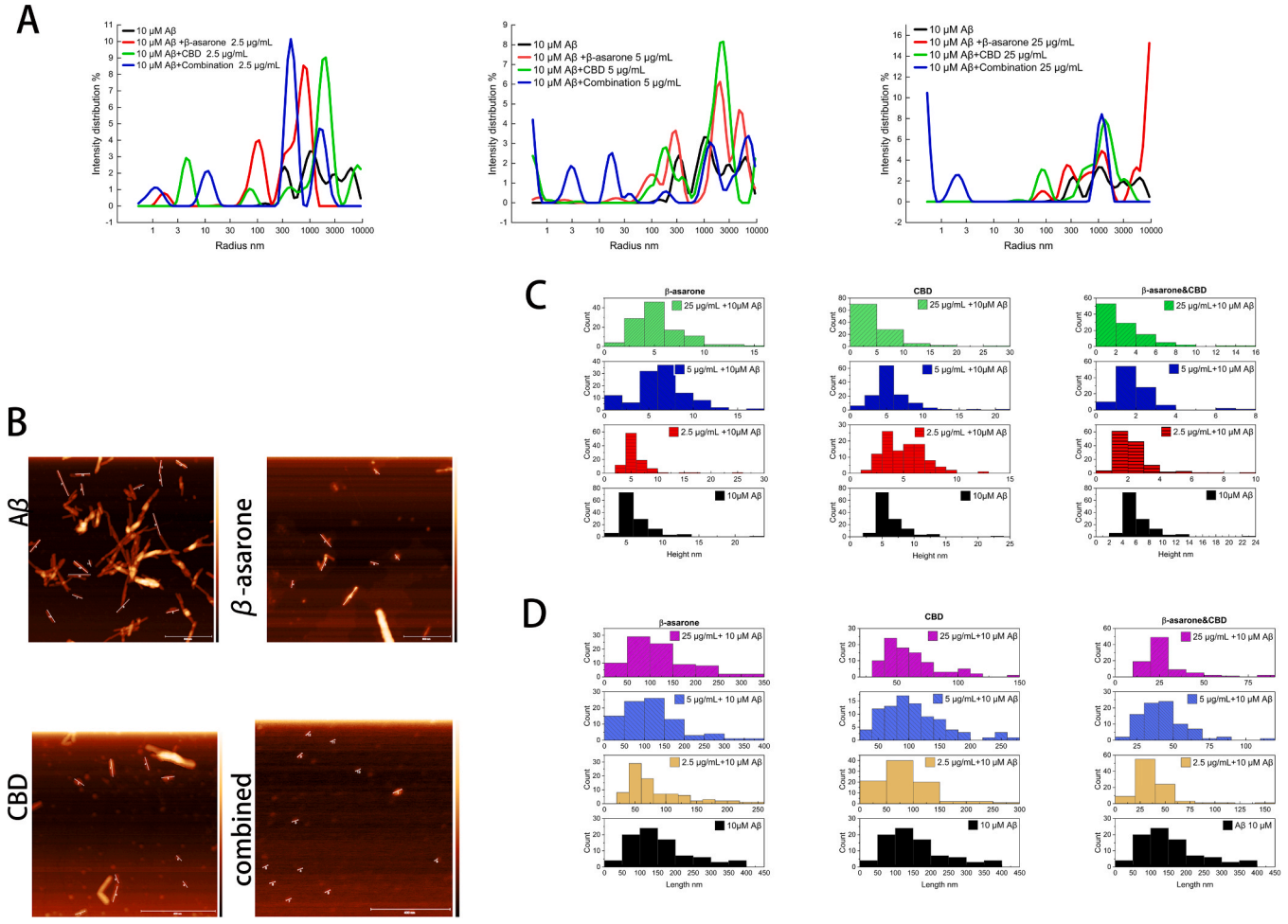

Fig. 2. β-asarone and CBD could inhibit Aβ aggregation confirmed by size distribution and the morphology of the mixture collected from ThT binding assay. (A) Scattering intensity of size distribution (diameter, d.nm). (B)Atomic force microscopy (AFM) images of Aβ incubated with different combination of the two phytochemicals (2.5 μg/mL of each). Scale bar for $A\beta_{40}$ and β-asarone is 500 nm, scale bar for CBD and combined group is 400 nm. (C) Height distributions of different concentritions. Samples range from 100 to 131. (D) Length distributions of different concentritions. Selected nanoparticles range from 84 to 94.

(Fig. 2A) of $A\beta_{40}$ showed a wide range broad size distribution range from 100 nm to 10,000 nm, the addition of β-asarone, CBD or the combination of them could influence the particle size. When the concentration was 2.5 μg/mL, β-asarone formed three predominant peaks and the majority peak (8 %) formed from 300 to 2000 nm. CBD group had three predominant peaks and the biggest peak (9 %) formed 1000–3000 nm. While combine them together, there would be four predominant peaks and the biggest peak (10 %) formed from 300 to 1000 nm. When the concentration was 5 μg/mL, β-asarone formed three predominant peaks ranging from 100 to 10,000 nm and the biggest peak (6 %) ranged from 1000–3000 nm. CBD formed two predominant peaks ranging from 100 to 3000 nm and the biggest peak (8 %) ranging from 1000 nm to 3000 nm. The combination group showed clear decrease on size and formed more smaller particles ranging from 1 to 100 nm and the ratios of different size distribution were all around 3 %. When the concentration was 25 μg/mL, β-asarone group and CBD group showed maintained the similar trend as the other concentration, and the combination group formed only two predominant peaks and the biggest one was 8 %. DLS results might be in accordance with ThT results that the combination treatment could decrease the fibril size. Although the sizes of fibril did not decrease clearly, while the particles tended to accumulate in some sizes instead of a wide range.

Samples were collected to further investigate the morphology of $A\beta_{40}$ affected by CBD, β-asarone and the combination of them. From ThT binding assay results, it seems that all the groups have reached to the same fluorescence signal, from AFM results (Fig. 2 B), it could be seen directly that what precisely we got after adding different phytochemical combinations. It was visually showed that, without any compound inside, after 16 h incubation, $A\beta_{40}$ was visually shown to form long fibers, whereas the addition of CBD and β-asarone has a profound effect on fibril formation.

Since AFM can provide the height and length information about the nanoparticles, so we first analyzed the height of the fibers (or aggregates) obtained from the ThT binding assay (Fig. 2C), and the overlapping regions were exclusive. We can see, the single use of either β-asarone or CBD could have visual influence on the height of the $A\beta_{40}$ aggregates, which has a predominant distribution around 5 nm. While when they work together, they could prominently decrease the height of the aggregates to 2 nm. The fiber length (Fig. 2 D) would more clearly show the conversion of Aβ fibrils into aggregates. Aβ fibers are 100–200 nm long, but can be shorter than 100 nm with β-asarone or CBD individually. If combine them, the length of the mixture could be around 20 – 30 nm when the concentration came to 25 μg/mL. Observations from AFM morphological images are consistent with the results of ThT binding assay and DLS analyses.

3.4. The combination treatment inhibits cell damage caused by APP/PS1 in vitro by decreasing the apoptosis

We also wanted to learn more about the combination of two phytochemicals acting on Aβ-induced apoptosis that we used *in vitro* and *in vivo* experiments. And *in vitro* experiment, we used only the low dosage group (either compound was 2.5 μg/mL) and medium dosage group (either compound was 5 μg/mL) of the combined dosages. The cells were first transfected with the plasmid overexpressed APP/PS1. Apoptosis is critical for normal development and tissue homeostasis, and plays an important role in cell development, differentiation, and balancing cell number in continued tissue regeneration and immune system development [56] and can be detected by probe [57,58]. In such condition, we used Annexin-V labeled by mCherry (Beyotime, Shanghai, China) to detect apoptosis. Annexin-V could selectively combine phosphatidylserine, which means the normal cells won't be stained by this red color. And the nuclei of the live cells were stained with the Hoechst 33342, to see further the apoptosis cells distribute in the live cells. In Fig. 3, in the control group the living cells were in clusters and less than in the other groups. When comparing the red to blue fluorescence intensity, the low concentration had the least ratio, which meant the cells were in a better situation than the others.

3.5. Combination treatment of the two phytochemicals alleviates the Aβ aggregation and enhances multiple behaviors in vivo

We used a higher concentration compared to *in vitro* experiments in wild type *C.elegans* N2 and Aβ over expressed strains (CL4176 and CL2355). The concentrations of the two phytochemicals were 100, 50 and 10 μg/mL at a ratio of 1:1. Firstly, we tested the basic behavior like pharyngeal pumping (Fig. 4 A). CBD had little influence on improving the pharyngeal pumping with different concentrations, while β-asarone could clearly increase the pharyngeal pumps, and when combined them in a medium dosage, the total pumps would be higher than separately

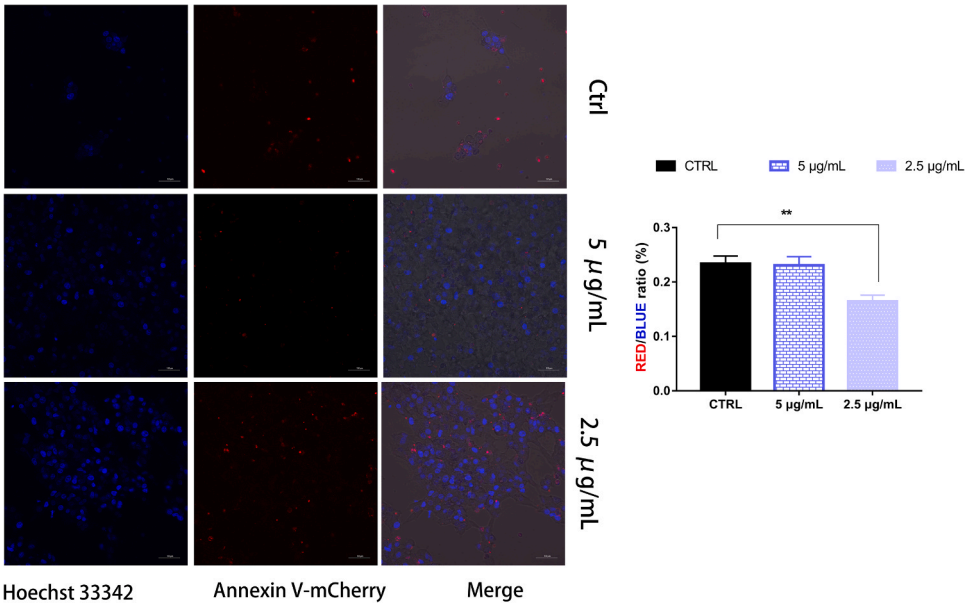

Fig. 3. Apoptosis in SH-SY5Y cell model. Cells were stained first by Annexin V-mCherry then were stained with Hoechst 33342. The ratio of Annexin V-mCherry and Hoechst 33342. Quantification was conducted with 9 replicates for each group and showed with mean ± SEM. *P < 0.05; **P < 0.01.

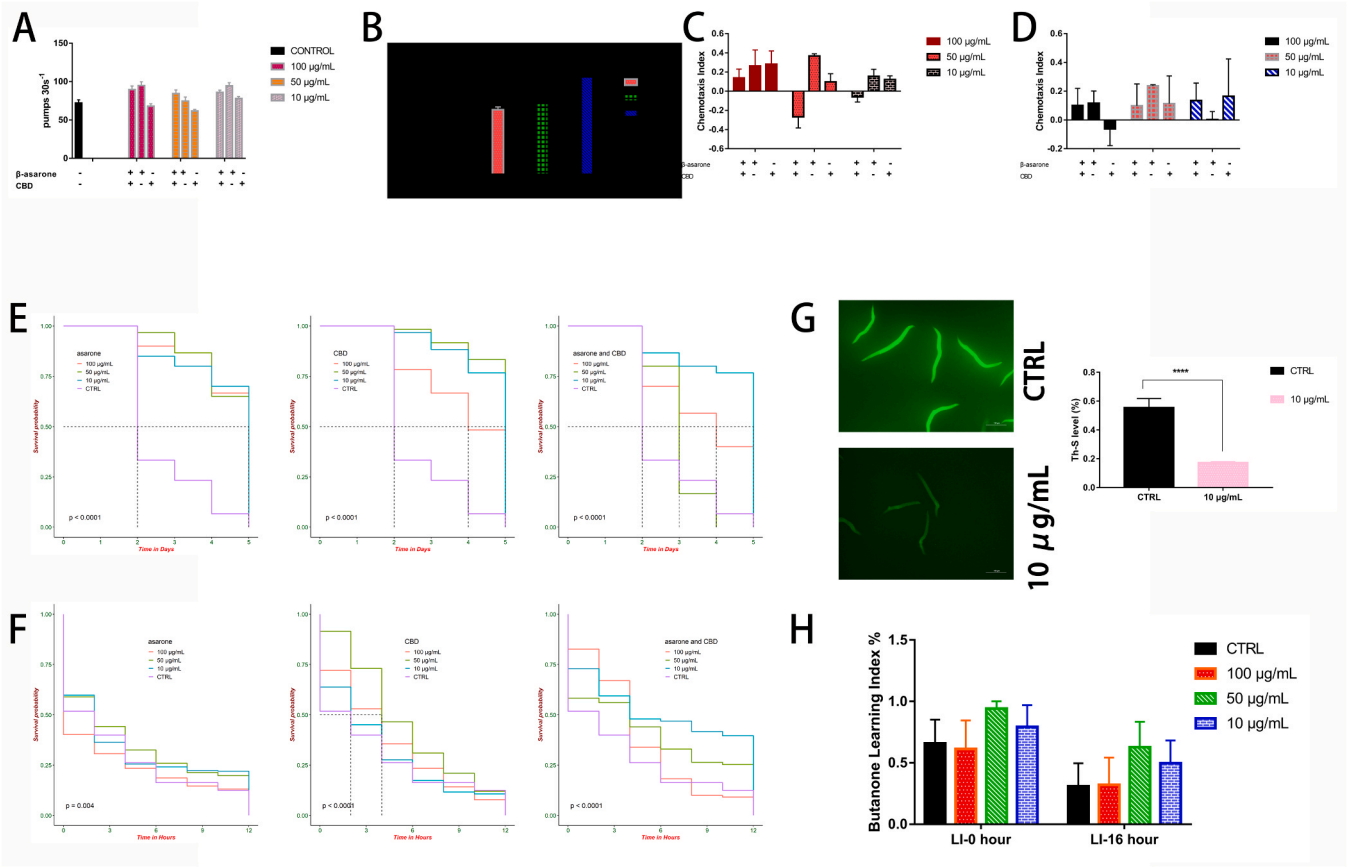

Fig. 4. *C.elegans* behavior results and Aβ expression with single or combined treatment of β-asarone and CBD. (A) Mean numbers of pharyngeal pumps. (B) Mean numbers of head thrashes. (C, D) Chemotaxis index for N2 and CL2355, respectively. (E) Paralysis curve shown non-paralyzed CL4176 worms after transferred to 25 °C at L4 stage with single or combined dosages and observed every day. (F) Paralysis curve shown non-paralyzed CL4176 worms after transferred to 25 °C at L3 stage with single or combined dosages and observed every 2 h. (G) ThS staining of CL4176 after transferred into 25 °C for 24 h to induce Aβ expression with combined treatment at a low dosage. (H) Learning index of N2 after long-term training for 0 h and 16 h, respectively.

use. The body binding assay result (Fig. 4 B) would clearly show that the low dosage of the combination treatment would hugely increase the body thresh hold counts, and it tended to have a negative dosage dependent trend. After that, we tested the chemotaxis index in N2 (Fig. 4 C) and CL2355 (Fig. 4 D) stains. In N2 group, β-asarone had a clear positive dosage dependent tendency, and CBD had a decrease when the dosage came to 50 μg/mL, while when combined them together, the chemotaxis index was lower than the single usage. In CL2355 group, it had more varies, CBD had a negative chemotaxis when the concentration came to 100 μg/mL, while β-asarone group would face the smallest chemotaxis index when the concentration came to 10 μg/mL.

If CL4176 were cultured at 25 °C could induce the expression of $A\beta_{1–42}$, which produces strong neurotoxicity will cause paralysis and shortened lifespan. To determine whether the combination treatment is able to alleviate the neurotoxicity caused by $A\beta_{1–42}$ in CL4176, we cultured the worms in the presence or absence of the 2 phytochemicals at different stage. While we found when the worms were transferred into higher temperature in L4 would have a longer period to paralyze when compared with L3. As shown in Fig. 4(E), the paralysis situation of CL4176 (L4) could be significantly extended in the presence of single β-asarone and CBD, particularly at the low and medium concentrations, while the combination treatment won't have a huge difference when compared to the single dosages. When the paralyze ended, the survival rate of the combined group (low dosage group) was over 75 %. The survival rates of the β-asarone groups were all around 75 %, and the survival rates of CBD groups with 10 μg/mL and 50 μg/mL were over 75 %, when the concentration reached 100 μg/mL, the survival rate would decrease to 50 %.

The results were consistent with those of paralysis tests initiated when the worms were at L3 (Fig. 4 F). After 12 h, the paralysis rates in the β-asarone and CBD groups were similar to the control group, with all rates being less than 25 %. However, combination treatment demonstrated superior antiparalytic activity. Interestingly, the combination of the two phytochemicals even showed a protective effect against $A\beta_{1–42}$ induced death at higher temperature, which was a harmful environment. At 12 h, the paralysis rate for the combined groups (low dosage group) was the only one to reach almost 50 % when compared to 10 % of that in the control group. The results indicated that the combination of the two phytochemicals was more helpful when the *C.elegans* experiment were performed at earlier stage (L3).

Next, we tested the Aβ aggregation status using the ThS staining method with combined treatment. We found that the low dosage group was able to significantly reduce Aβ aggregation compared with the control group (Fig. 4 G). The results also suggest that CL2355 may not be suitable for conducting long-term learning studies of these two phytochemicals. Therefore, the researchers used N_2 alone for long-term butanone training, which showed that the combined treatment significantly improved the learning index of N_2 after seven training sessions. However, after 16 h, the learning index of the intermediate group still remained the best, almost 30 % higher than the control group. These findings suggest that the combination treatment of β-asarone and CBD may have potential for improving learning and memory in AD.

3.6. The combination treatment decreases the apoptosis caused by Aβ in vivo

In vivo experiments assessing apoptotic status were conducted in the control group (treated with DMSO 0.4 %) and the low dosage group (10 μg/mL for each phytochemical). In *C.elegans*, aggregated Aβ can cause significant neuronal damage [32] with the nerve ring located close to the mouth being part of ganglia and easily quantifiable. To assess mitochondrial apoptosis, JC-1 was used, which aggregates within the matrix and turns red at high potentials and green at lower potentials. The red-to-green ratio likely reflects mitochondrial apoptosis, and it was found that the strength of this ratio was significantly reduced. Our results suggest that combination treatment could reverse Aβ-induced apoptosis *in vivo* (Fig. 5), as evidenced by an increase in the red/green ratio by almost 44 % when compared to the control group.

4. Discussion

The objective of this study was to develop a potential way to combine the two phytochemicals. We first tested the ability of the phytochemicals to inhibit $A\beta_{40}$ aggregation *in vitro* and found that β-asarone and CBD at a concentration of 2.5 μg/mL had a superior inhibitory effect. The inhibitory activity of them were not all dosage-dependent. We analyzed the differentially expressed genes (DEGs) from a database (GSE97760) and retrograde endocannabinoid signal pathway using various bioinformatics methods, and selected six genes for gene expression analysis to determine how the combination of the two compounds had an effect on these genes. Our results were further confirmed through DLS size distribution analysis and AFM morphology images. The DLS results showed that when the two compounds were combined, the aggregation of $A\beta_{40}$ was interrupted and more smaller size particles formed. The AFM images visually presented the particles' internal structure, and we randomly selected dozens of particles from different areas on the mica to perform a statistical analysis of their height and length distributions. The morphology analysis confirmed that both β-asarone and CBD could inhibit $A\beta_{40}$ aggregation, mainly by inhibiting fiber length formation. Furthermore, the combination of the two phytochemicals could reduce fiber formation in both height and length dimensions.

To further investigate the potential of our phytochemicals, we constructed a cell model that can express APP/PS1. After transfection, the cells received different concentration of the two phytochemicals. In pilot experiments, we found that concentrations higher than 25 μg/mL of either compound were toxic to the cells. Therefore, in the subsequent *in vitro* experiments, we used only two different concentrations. We observed that even the low-dosage combination (2.5 μg/mL of each) was able to maintain cell morphology and reverse the transfection-induced side effects. Moreover, the dosage was lower than that used in a previous study [59], which employed 7 μg/mL of β-asarone to improve cell viability. From the cell viability experiment, we could observe that the high concentration of CBD would be toxic to cells and β-asarone could reverse the harm, which make this combination more friendly to *in vivo* experiment in the near future.

Combination treatment has been successful in treating various disease, including cancer and human immunodeficiency virus 1 (HIV). This approach may prove to be more effective than targeting only one mechanism at a time [36]. Currently, research on combing CBD with other cannabinoids for AD treatment is limited. However, there have been positive results when THC and CBD were combined in the CREAE model of spasticity in multiple sclerosis (MS) [60]. Additionally, studies have shown that THC and CBD can alter the gut microbiome [61]. A previous study [16] examined the effects of combining β-asarone with icariin to inhibit Aβ. Similarly, our research aimed to overcome the limitations of using single compounds by combining β-asarone and CBD to achieve lower effective doses and better results. Our findings showed that β-asarone and CBD delayed $A\beta_{40}$ aggregation, and the combination was effective at lower doses. We confirmed that the selected doses were able to reverse Aβ-induced side effects and suppress upregulated genes in the blood of AD patients in cells treated with the β-asarone and CBD combination. Besides, the addition of β-asarone could also be possible attenuate the toxicity caused by CBD.

Aging-related dysfunction of autophagy and subsequent metabolic or oxidative stress can lead to the accumulation of indigestible or incompletely degraded substances, such as APP and its processing enzyme [62,63]. Several studies have demonstrated that promoting mitochondrial autophagy can improve the cognitive deficits associated with Aβ and tau pathologies [64]. The expression of autophagy-related proteins was confirmed in cell models treated with CBD and β-asarone. These models showed a decreased intensity of LC3II / I and Bcl-xl compared to the untreated control group. Our results suggest that the CBD may have contributed to the inhibition of P62 expression.

Aβ was found to induce apoptosis [65]. The findings suggest that the combination of CBD and β-asarone may have therapeutic potential in

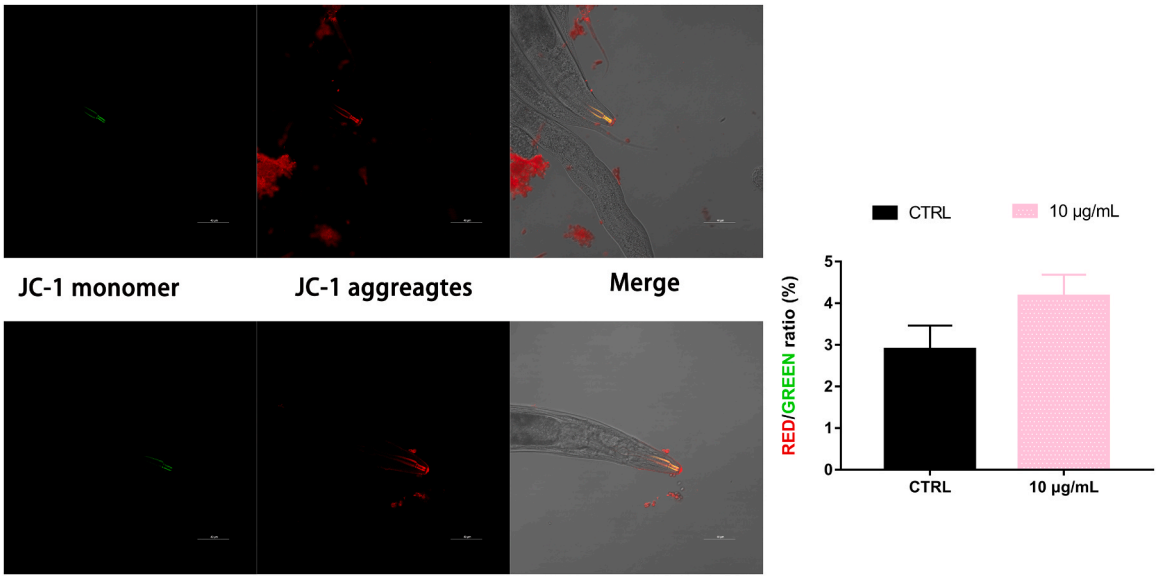

Fig. 5. CL 4176 worms were hybrid with JC-1 for 1 h to test the fluorescence in the nerve ring. The upper row was the control group, the lower row was combination group with 10 μg/mL for each compound. Scale bar is 150 μm. Quantification was conducted with 15 replicates.

treating Alzheimer's disease by promoting autophagy and inhibiting apoptosis. In addition, the downregulation of genes upregulated in AD patients' blood suggests that the combination treatment may have a systemic effect in improving the overall health of AD patients. The use of blood samples as a method to demonstrate the process also provides a non-invasive and convenient approach for monitoring the efficacy of the treatment. Further studies, including animal studies and clinical trials, are needed to validate these findings and assess the safety and efficacy of the combination treatment in treating Alzheimer's disease.

Taken together, our results demonstrate that the combination of β-asarone and CBD reduces $A\beta_{40}$ aggregation and increases learning activity. This study provides a new perspective on the potential of β-asarone and CBD for Aβ. And in the future, we may focus on the initial mechanism of the two phytochemicals work on the AD related proteins and how these protein structures change.

However, these results also remain some questions needed to be answered in the near future, such as, (1) if the two components interact with each other before link to Aβ? (2) will the combination of them will have a long period influence after dosage? (3) if different ratios of the two phytochemicals have more efficient effect?

Author contribution

Fangyuan Duan performed the experimnets and conceived the study, Ting Ju involved in cell culture and transfection experimens, Chen Song involved in methodology, Mengyao Liu and Yi Xiong involved in *C.elegnas* experiments, Jinghui Luo involved in getting access to AFM and DLS equipment, Xue Han and Weihong Lu involved in modification.

Declaration of Competing Interest

The authors declare the following financial interests/personal relationships which may be considered as potential competing interests: Weihong Lu reports financial support, article publishing charges, equipment, drugs, or supplies, statistical analysis, and writing assistance were provided by National Key Research and Development Program of China. Weihong Lu reports financial support was provided by Heilongjiang Touyan Team. Fangyuan Duan reports a relationship with China Scholarship Council that includes: funding grants.

Acknowledgements

We would like to thank Jinghui Luo providing technical help. This research was supported by the National Key Research and Development Program of China (2017YFC160900), Heilongjiang Touyan Team (HITTY-20190034), China Scholarship Council (202106120270).

Appendix A. Supporting information

Supplementary data associated with this article can be found in the online version at doi:10.1016/j.csbj.2023.07.028.

References

[1] Jung H, Lee SY, Lim S, Choi HR, Choi Y, Kim M, et al. Anti-inflammatory clearance of amyloid-β by a chimeric Gas6 fusion protein. Nat Med 2022;28(9). 1802-12.
[2] Ossenkoppele R, Pichet Binette A, Groot C, Smith R, Strandberg O, Palmqvist S, et al. Amyloid and tau PET-positive cognitively unimpaired individuals are at high risk for future cognitive decline. Nat Med 2022;28(11):2381–7.
[3] Ghosh AK, Osswald HL. BACE1 (β-secretase) inhibitors for the treatment of Alzheimer's disease. Chem Soc Rev 2014;43(19):6765–813.
[4] Hur JY, Frost GR, Wu X, Crump C, Pan SJ, Wong E, et al. The innate immunity protein IFITM3 modulates γ-secretase in Alzheimer's disease. Nature 2020;586 (7831):735–40.
[5] Da Mesquita S, Papadopoulos Z, Dykstra T, Brase L, Farias FG, Wall M, et al. Meningeal lymphatics affect microglia responses and anti-Aβ immunotherapy. Nature 2021;593(7858):255–60.
[6] Woodruff-Pak DS, Tobia MJ, Jiao X, Beck KD, Servatius RJ. Preclinical investigation of the functional effects of memantine and memantine combined with galantamine or donepezil. Neuropsychopharmacol: Publ Am Coll Neuropsychopharmacol 2007;32(6):1284–94.
[7] Lorrio S, Negredo P, Roda JM, García AG, López MG. Effects of memantine and galantamine given separately or in association, on memory and hippocampal neuronal loss after transient global cerebral ischemia in gerbils. Brain Res 2009; 1254:128–37.
[8] Peng J, Fan M, An C, Ni F, Huang W, Luo J. A narrative review of molecular mechanism and therapeutic effect of cannabidiol (CBD). Basic Clin Pharmacol Toxicol 2022;130(4):439–56.
[9] Chesworth R, Cheng D, Staub C, Karl T. Effect of long-term cannabidiol on learning and anxiety in a female Alzheimer's disease mouse model. Front Pharm 2022;13: 931384.
[10] Dávila EM, Patricio F, Rebolledo-Bustillo M, Garcia-Gomez D, Hernandez JCG, Sanchez-Gaytan BL, et al. Interacting binding insights and conformational consequences of the differential activity of cannabidiol with two endocannabinoid-activated G-protein-coupled receptors. Front Pharm 2022;13:945935.
[11] Wang N, Wang H, Li L, Li Y, Zhang R. β-Asarone inhibits Amyloid-β by promoting autophagy in a cell model of Alzheimer's disease. Front Pharm 2019;10:1529.
[12] Meng M, Zhang L, Ai D, Wu H, Peng W. β-Asarone ameliorates β-amyloid-induced neurotoxicity in PC12 cells by activating P13K/Akt/Nrf2 signaling pathway. Front Pharm 2021;12:659955.
[13] Huang L, Deng M, Zhang S, Lu S, Gui X, Fang Y. β-asarone and levodopa coadministration increases striatal levels of dopamine and levodopa and improves behavioral competence in Parkinson's rat by enhancing dopa decarboxylase activity. Biomed Pharmacother = Biomedecine Pharmacother 2017;94:666–78.
[14] Huang L, Deng M, Zhang S, Fang Y, Li L. Coadministration of β-asarone and levodopa increases dopamine in rat brain by accelerating transformation of levodopa: a different mechanism from Madopar. Clin Exp Pharmacol Physiol 2014; 41(9):685–90.
[15] Huang L, Deng M, He Y, Lu S, Ma R, Fang Y. β-asarone and levodopa co-administration increase striatal dopamine level in 6-hydroxydopamine induced rats by modulating P-glycoprotein and tight junction proteins at the blood-brain barrier and promoting levodopa into the brain. Clin Exp Pharmacol Physiol 2016; 43(6):634–43.
[16] Wang N, Wang H, Pan Q, Kang J, Liang Z, Zhang R. The combination of β-asarone and icariin inhibits amyloid-β and reverses cognitive deficits by promoting mitophagy in models of Alzheimer's disease. Oxid Med Cell Longev 2021;2021: 7158444.
[17] Dong H, Wu S, Hu N, Xing G. Efficacy of tenuigenin and β-asarone as augmentations for memantine in the treatment of Alzheimer's disease. Neuroreport 2018;29(3):203–7.
[18] Liang ZH, Cheng XH, Ruan ZG, Wang H, Li SS, Liu J, et al. Protective effects of components of the Chinese herb grassleaf sweetflag rhizome on PC12 cells incubated with amyloid-beta42. Neural Regen Res 2015;10(8):1292–7.
[19] Caldwell KA, Willicott CW, Caldwell GA. Modeling neurodegeneration in Caenorhabditis elegans. Dis Models Mech 2020;13(10).
[20] Zhang ZP, Bai X, Cui WB, Chen XH, Liu X, Zhi DJ, et al. Diterpenoid Caesalmin C delays Aβ-induced paralysis symptoms via the DAF-16 pathway in Caenorhabditis elegans. Int J Mol Sci 2022;23(12).
[21] Oliveira BSA, Milanezi DS, Gonzaga PDV, Detoni FR, Soriano RN. The gut microbiota in neurodegenerative diseases: revisiting possible therapeutic targets for cannabidiol. Heliyon 2022;8(12):e12172.
[22] Townsend M, Shankar GM, Mehta T, Walsh DM, Selkoe DJ. Effects of secreted oligomers of amyloid beta-protein on hippocampal synaptic plasticity: a potent role for trimers. J Physiol 2006;572(Pt 2):477–92.
[23] Cooray R, Gupta V, Suphioglu C. Current aspects of the endocannabinoid system and targeted THC and CBD phytocannabinoids as potential therapeutics for Parkinson's and Alzheimer's diseases: a review. Mol Neurobiol 2020;57(11): 4878–90.
[24] Liang AL, Gingher EL, Coleman JS. Medical cannabis for gynecologic pain conditions: a systematic review. Obstet Gynecol 2022;139(2):287–96.
[25] Penazzi L, Lorengel J, Sündermann F, Golovyashkina N, Marre S, Mathis CMB, et al. DMSO modulates CNS function in a preclinical Alzheimer's disease model. Neuropharmacology 2017;113(Pt A):434–44.
[26] Lin CK, Kalunta CI, Chen FS, Nguyen TT, Kaptein JS, Lad PM. Dimethyl sulfoxide suppresses apoptosis in Burkitt's lymphoma cells. Exp Cell Res 1995;216(2): 403–10.
[27] Hanslick JL, Lau K, Noguchi KK, Olney JW, Zorumski CF, Mennerick S, et al. Dimethyl sulfoxide (DMSO) produces widespread apoptosis in the developing central nervous system. Neurobiol Dis 2009;34(1):1–10.
[28] Kang MH, Das J, Gurunathan S, Park HW, Song H, Park C, et al. The cytotoxic effects of dimethyl sulfoxide in mouse preimplantation embryos: a mechanistic study. Theranostics 2017;7(19):4735–52.
[29] Brenner S. The genetics of Caenorhabditis elegans. Genetics 1974;77(1):71–94.
[30] Oakley H, Cole SL, Logan S, Maus E, Shao P, Craft J, et al. Intraneuronal beta-amyloid aggregates, neurodegeneration, and neuron loss in transgenic mice with five familial Alzheimer's disease mutations: potential factors in amyloid plaque formation. J Neurosci: J Soc Neurosci 2006;26(40):10129–40.
[31] de Felipe P, Luke GA, Hughes LE, Gani D, Halpin C, Ryan MD. E unum pluribus: multiple proteins from a self-processing polyprotein. Trends Biotechnol 2006;24 (2):68–75.
[32] Yang T, Zhao X, Zhang Y, Xie J, Zhou A. 6‴-Feruloylspinosin alleviated beta-amyloid induced toxicity by promoting mitophagy in Caenorhabditis elegans (GMC101) and PC12 cells. Sci Total Environ 2020;715:136953.
[33] Li X, Wang X, Wang K, Yang X, Liu X, Chen J, et al. Black rice anthocyanin extract enhances the antioxidant capacity in PC12 cells and improves the lifespan by

activating IIS pathway in Caenorhabditis elegans. Comp Biochem Physiol Toxicol Pharm: CBP 2022;265:109533.
[34] Qin Y, Chen F, Tang Z, Ren H, Wang Q, Shen N, et al. Ligusticum chuanxiong Hort as a medicinal and edible plant foods: antioxidant, anti-aging and neuroprotective properties in Caenorhabditis elegans. Front Pharm 2022;13:1049890.
[35] Johnson JR, Ferdek P, Lian LY, Barclay JW, Burgoyne RD, Morgan A. Binding of UNC-18 to the N-terminus of syntaxin is essential for neurotransmission in Caenorhabditis elegans. Biochem J 2009;418(1):73–80.
[36] Margie O, Palmer C, Chin-Sang I. C. elegans chemotaxis assay. J Vis Exp: JoVE 2013;74:e50069.
[37] Kauffman A, Parsons L, Stein G, Wills A, Kaletsky R, Murphy C. C. elegans positive butanone learning, short-term, and long-term associative memory assays. J Vis Exp: JoVE 2011;(49)).
[38] Zhao L, Duan Z, Wang Y, Wang M, Liu Y, Wang X, et al. Protective effect of Terminalia chebula Retz. extract against Aβ aggregation and Aβ-induced toxicity in Caenorhabditis elegans. J Ethnopharmacol 2021;268:113640.
[39] Stiernagle T. Maintenance of C. elegans. WormBook: the online review of C elegans biology. 2006. p. 1–11.
[40] Yang T, Zhao X, Zhang Y, Xie J, Zhou A. 6‴-Feruloylspinosin alleviated beta-amyloid induced toxicity by promoting mitophagy in Caenorhabditis elegans (GMC101) and PC12 cells. Sci Total Environ 2020;715:136953.
[41] Usov I, Adamcik J, Mezzenga R. Polymorphism complexity and handedness inversion in serum albumin amyloid fibrils. ACS Nano 2013;7(12):10465–74.
[42] Nečas D, Klapetek P. Gwyddion: an open-source software for SPM data analysis. Cent Eur J Phys 2012;10(1):181–8.
[43] Ramesh M, Acharya A, Murugan NA, Ila H, Govindaraju T. Thiophene-based dual modulators of Aβ and tau aggregation. Chembiochem: A Eur J Chem Biol 2021;22 (23):3348–57.
[44] Wu J, Österlund N, Wang H, Sternke-Hoffmann R, Pupart H, Ilag LL, et al. Identifying the role of co-aggregation of Alzheimer's amyloid-β with amorphous protein aggregates of non-amyloid proteins. Cell Rep Phys Sci 2022;3(9):101028.
[45] Willander H, Presto J, Askarieh G, Biverstål H, Frohm B, Knight SD, et al. BRICHOS domains efficiently delay fibrillation of amyloid β-peptide. J Biol Chem 2012;287 (37):31608–17.
[46] Meisl G, Kirkegaard JB, Arosio P, Michaels TCT, Vendruscolo M, Dobson CM, et al. Molecular mechanisms of protein aggregation from global fitting of kinetic models. Nat Protoc 2016;11(2):252–72.
[47] Xicoy H, Wieringa B, Martens GJ. The SH-SY5Y cell line in Parkinson's disease research: a systematic review. Mol Neurodegener 2017;12(1):10.
[48] Glenner GG, Wong CW. Alzheimer's disease: initial report of the purification and characterization of a novel cerebrovascular amyloid protein. Biochem Biophys Res Commun 1984;120(3):885–90.
[49] Nixon RA, Wegiel J, Kumar A, Yu WH, Peterhoff C, Cataldo A, et al. Extensive involvement of autophagy in Alzheimer disease: an immuno-electron microscopy study. J Neuropathol Exp Neurol 2005;64(2):113–22.
[50] Yu WH, Cuervo AM, Kumar A, Peterhoff CM, Schmidt SD, Lee JH, et al. Macroautophagy–a novel Beta-amyloid peptide-generating pathway activated in Alzheimer's disease. J Cell Biol 2005;171(1):87–98.
[51] Zhang Z, Yang X, Song YQ, Tu J. Autophagy in Alzheimer's disease pathogenesis: Therapeutic potential and future perspectives. Ageing Res Rev 2021;72:101464.
[52] Luo R, Su LY, Li G, Yang J, Liu Q, Yang LX, et al. Activation of PPARA-mediated autophagy reduces Alzheimer disease-like pathology and cognitive decline in a murine model. Autophagy 2020;16(1):52–69.
[53] Bailus BJ, Scheeler SM, Simons J, Sanchez MA, Tshilenge KT, Creus-Muncunill J, et al. Modulating FKBP5/FKBP51 and autophagy lowers HTT (huntingtin) levels. Autophagy 2021;17(12):4119–40.
[54] Deng M, Huang L, Zhong X. β-asarone modulates Beclin-1, LC3 and p62 expression to attenuate Aβ40 and Aβ42 levels in APP/PS1 transgenic mice with Alzheimer's disease. Mol Med Rep 2020;21(5). 2095-102.
[55] Wang Z, Zheng P, Chen X, Xie Y, Weston-Green K, Solowij N, et al. Cannabidiol induces autophagy and improves neuronal health associated with SIRT1 mediated longevity. GeroScience 2022.
[56] Kurowska P, Mlyczynska E, Rak A. Effect of ghrelin on the apoptosis of various cells. A critical review. J Physiol Pharm: J Pol Physiol Soc 2019;70(1).
[57] Vermes I, Haanen C, Steffens-Nakken H, Reutelingsperger C. A novel assay for apoptosis. Flow cytometric detection of phosphatidylserine expression on early apoptotic cells using fluorescein labelled Annexin V. J Immunol Methods 1995;184 (1):39–51.
[58] Tan Z, Xiao L, Tang M, Bai F, Li J, Li L, et al. Targeting CPT1A-mediated fatty acid oxidation sensitizes nasopharyngeal carcinoma to radiation therapy. Theranostics 2018;8(9). 2329-47.
[59] Xue Z, Guo Y, Zhang S, Huang L, He Y, Fang R, et al. Beta-asarone attenuates amyloid beta-induced autophagy via Akt/mTOR pathway in PC12 cells. Eur J Pharmacol 2014;741:195–204.
[60] Hilliard A, Stott C, Wright S, Guy G, Pryce G, Al-Izki S, et al. Evaluation of the effects of sativex (THC BDS: CBD BDS) on inhibition of spasticity in a chronic relapsing experimental allergic autoimmune encephalomyelitis: a model of multiple sclerosis. ISRN Neurol 2012;2012:802649.
[61] Al-Ghezi ZZ, Busbee PB, Alghetaa H, Nagarkatti PS, Nagarkatti M. Combination of cannabinoids, delta-9-tetrahydrocannabinol (THC) and cannabidiol (CBD), mitigates experimental autoimmune encephalomyelitis (EAE) by altering the gut microbiome. Brain Behav Immun 2019;82:25–35.
[62] Steele JW, Lachenmayer ML, Ju S, Stock A, Liken J, Kim SH, et al. Latrepirdine improves cognition and arrests progression of neuropathology in an Alzheimer's mouse model. Mol Psychiatry 2013;18(8):889–97.
[63] Zare-Shahabadi A, Masliah E, Johnson GV, Rezaei N. Autophagy in Alzheimer's disease. Rev Neurosci 2015;26(4):385–95.
[64] Fang EF, Hou Y, Palikaras K, Adriaanse BA, Kerr JS, Yang B, et al. Mitophagy inhibits amyloid-β and tau pathology and reverses cognitive deficits in models of Alzheimer's disease. Nat Neurosci 2019;22(3). 401-12.
[65] Hwang S, Lim JW, Kim H. Inhibitory effect of lycopene on amyloid-β-induced apoptosis in neuronal cells. Nutrients 2017;9(8).